Smart Footstep Energy Generation Using Piezoelectric Sensors, Energy Management, And IoT Monitoring

Venumadhava M[1], A. Jeeva[2], Chandru. N[3], J. Sandeep[4], P.V Sudarshan Rao[5]
[1,2,3,4,5]*Department of Computer Science, Artificial Intelligence and Machine Learning, PDIT, Hosapete, India*

***Abstract*—This paper presents a smart floor-tile architecture that converts intermittent human-footstep excitation into buffered electrical energy while exposing its operating state through an Internet of Things (IoT) dashboard. The proposed design couples a mechanically protected piezoelectric array with a low-loss bridge rectifier, transient clamp, storage interface, lithium-ion buffer, ESP32 controller, and cloud telemetry. Rather than treating a high open-circuit voltage as useful power, the design evaluates the complete energy path: source impedance, rectifier loss, storage acceptance, quiescent consumption, and load scheduling. An edge-resident energy-management policy estimates the energy available per event, predicts near-term footfall intensity from recent inter-arrival statistics, and authorizes noncritical loads only when a state-of-charge reserve is maintained. The IoT layer samples rectified voltage, storage voltage, and load current; it uploads filtered features and retains local summaries during network outages. A mathematical model links stress-induced charge, capacitance, load resistance, and energy accumulated in the buffer. Since the supplied project report does not contain calibrated bench measurements, the results section is explicitly presented as an analytical validation case and repeatable experimental protocol rather than as a claim of measured field performance. The resulting system is appropriate for educational prototypes and low-duty-cycle sensing or indication in high-footfall sites; it is not proposed as a substitute for grid energy.**

***Index Terms*—piezoelectric energy harvesting, footstep energy, ESP32, Internet of Things, energy management, smart flooring.**

I. INTRODUCTION

Unlike solar or wind systems, footstep harvesters are coupled to human traffic and therefore inherit its randomness. The source has periods of high excitation followed by long silent intervals. An effective design stores impulses, sleeps the controller, and provides a useful function even when the recovered energy cannot meet all electronic demand. This premise guides the scope of the paper: it addresses a tile-level platform for edge sensing and small indication loads, not a comparison with utility-scale renewable generation.

Pedestrian motion is a distributed mechanical resource that is generally dissipated in floor compliance and footwear. Piezoelectric flooring offers a way to transduce a small fraction of this energy into electrical charge. Its most credible role is not bulk electricity generation, but autonomous sensing, local visual indication, and data-rich smart-infrastructure services [1]-[4]. Recent work on human-trampling harvesters highlights that mechanical packaging, converter loss, and the duty cycle of electronics are decisive to usefulness [1], [5]. This paper extends the base concept in the supplied project report by defining a publication-oriented architecture that includes measured-quantity discipline, energy-aware AI control, and a failure-tolerant IoT workflow.

The contributions are: (i) a complete hardware and data-path architecture; (ii) a lightweight energymanagement workflow suited to an ESP32; (iii) equations for source, power, and stored-energy estimation; and (iv) a reproducible validation plan and analytical results that do not overstate the available evidence.

II. LITERATURE SURVEY

A second stream of literature concerns sensing rather than energy supply. In smart-floor applications, the same mechanical pulse can be used for occupancy counting, gait-related event classification, and facility analytics. That dual role is valuable because it permits

a tile to justify its electronics through information value even where recoverable energy is modest. However, it also introduces a methodological obligation: sensing accuracy, harvested energy, and controller consumption must be reported separately. Conflating them makes inter-study comparisons unreliable.

Recent reviews further identify durability and user comfort as adoption constraints. A floor tile must remain slip-resistant, tolerate off-axis loading, resist moisture ingress, and avoid a perceptible stroke that changes walking behavior [1], [23]. Accordingly, the present design uses a mechanically protected and serviceable array. Its novelty is system-level coordination: the energy budget, dashboard duty cycle, and local load are governed together rather than treated as independent demonstrations.

The converter is another major source of variation in published results. Conventional diode bridges are robust and easy to explain, but their forward loss reduces transferred charge during small events. Voltage doublers can improve the available DC level under particular conditions, while synchronized switching interfaces may improve extraction but introduce control complexity [6], [8]-[10]. A publishable comparison should describe the exact conditioning topology and its input and output measurement points. Without this information, reported voltage peaks cannot be used to infer delivered energy.

IoT energy-monitoring studies contribute useful practices for remote observability, including timestamped data, cloud visualization, and fault alarms. Their usual energy assumption is a stable solar, mains, or battery supply. A footstep tile differs because telemetry may be the dominant load. This distinction motivates a controller that treats networking as a scheduled service. The literature therefore supports an integrated design question: how should the system spend scarce recovered energy while retaining a trustworthy record of its own behavior?

Energy-harvesting floors have been implemented with piezoelectric beams, disks, electromagnetic mechanisms, and hybrid transducers. 2022 review catalogues available smart-floor technologies and emphasizes that reported output depends strongly on stroke, mechanical transmission, and test procedure [1]. A multi-layer beam floor demonstrated the value of strain distribution and structural comparison [5], while a 2023 IEEE footstepfloor study reported a 405 mm tile and a maximum harvested power of 249.6 mW using a voltage-doubler extraction stage [6]. Recent IoT-oriented work combines footfall sensing, energy harvesting, and anomaly detection, but also makes clear that auxiliary power can be required in practical deployments [7].

The research gap is therefore an operational one: the energy source is irregular, whereas Wi-Fi communication and cloud dashboards impose bursty consumption. General piezoelectric interface research recommends matching the rectifier, storage element, and duty cycle to the source rather than optimizing a sensor in isolation [8][10]. The proposed system applies this principle by allowing the controller to defer cloud transmission and discretionary loads when energy reserve is low.

III. PROPOSED METHODOLOGY

Design begins with site characterization. The installer records peak-hour footfall, typical shoe contact region, available tile depth, exposure to moisture, and the function to be supported. A busy entrance may prioritize count accuracy and visible feedback; a corridor may prioritize low-duty-cycle beacon power. This information sets the number of piezo groups, required storage capacity, and the reserve threshold. A site with insufficient traffic should retain the sensing function but provision an auxiliary supply rather than overstate harvesting capability.

The mechanical stack is designed to distribute force while limiting excessive ceramic strain. A rigid upper plate provides user-facing durability; an elastomeric layer reduces local point loads; and a lower support defines the allowable displacement. Electrical wiring is strainrelieved and routed away from high-compression zones. This layout protects both the transducer and the connection reliability that is often neglected in desktop demonstrations.

Commissioning consists of a mechanical and electrical acceptance sequence. First, inspect displacement and rebound under a calibrated load; second, verify the clamp voltage with the storage path disconnected; third, measure the bridge and charger transfer into a known capacitive or resistive load; and fourth, enable the controller and compare reported values against instruments. Versioned firmware, a device

configuration record, and a fixed test script make later comparisons repeatable.

The electrical characterization begins by measuring the bare piezo group with a high-impedance instrument, then repeats the test with a known resistive load, the rectifier, the reservoir, and the storage interface. Each additional stage exposes loss or impedance mismatch. The same mechanical input is used for all stages. This staged method is preferable to recording only a final LED response, because it identifies whether a poor result arises from the transducer, mechanics, converter, wiring, or charger.

The tile should have an installation envelope that is explicit in the paper: active-area dimensions, total height, allowable displacement, maximum recommended force, sealing concept, cable egress, and service access. A simple bill of materials may be included in an appendix during submission. These practical details matter for real floor use, where installation and maintenance commonly determine viability more than an isolated electrical peak.

A modular tile contains a top plate, compliant forcespreading layer, piezoelectric sub-array, bottom support, and serviceable electronics enclosure. The sub-array is wired in series-parallel groups: series connection raises the available voltage for cold-start and rectification, whereas parallel connection increases charge capacity. Each group is protected by a clamp so that unusually strong impact does not exceed the converter or ADC input range. The rectified output feeds a reservoir capacitor and a controlled storage path. The ESP32 is powered from the battery rail rather than directly from the piezoelectric signal, preventing resets during sparse traffic.

The methodology has four loops: harvesting and protection; measurement and filtering; energy-aware control; and telemetry. It distinguishes the energyharvesting path from the monitoring path, because an ESP32 Wi-Fi transmit burst can consume more energy than several low-force events provide. The platform should therefore be installed where footfall is high enough to justify its sensing and educational value, with a small supplementary source only when continuous connectivity is required.

IV. SYSTEM ARCHITECTURE

The architecture deliberately creates three electrical domains: an unregulated pulse domain, a protected storage domain, and a regulated digital domain. The pulse domain may show high instantaneous voltage and must never be connected directly to an ESP32 pin. The storage domain incorporates reverse-current blocking and cell protection. The digital domain is regulated, decoupled, and switched or slept between samples. This partitioning makes troubleshooting tractable: a harvesting problem, charging problem, and telemetry problem can each be diagnosed without loading the other domains.

At the software boundary, the firmware is organized as a sampler, estimator, scheduler, communications client, and health monitor. The sampler has the highest priority during an event. The estimator converts readings to physical units and tracks energy. The scheduler decides whether to display, upload, or sleep. The communications client is deliberately decoupled so a blocked network request never interrupts energy capture. This separation allows each unit to be tested with recorded traces.

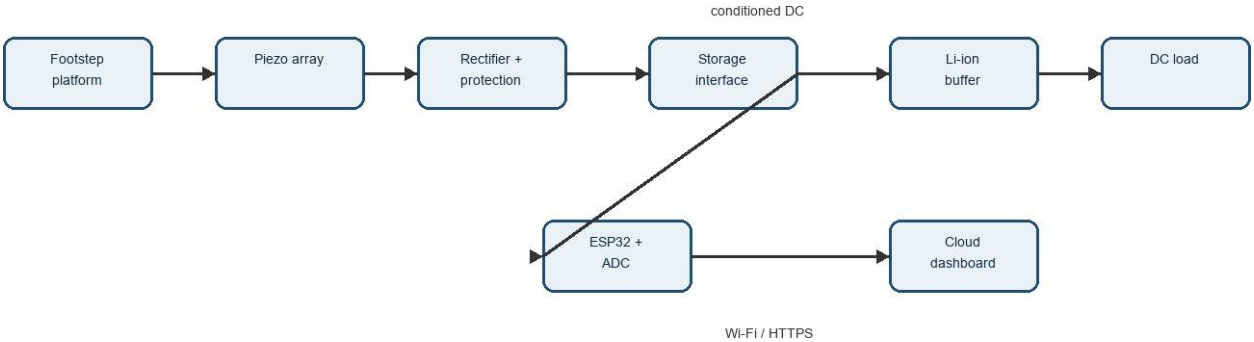


Fig. 1. Proposed energy, control, and telemetry architecture.

The power path terminates at the buffer and low-power load. In parallel, a resistor divider measures the rectified rail and battery voltage; an isolated or Hall-effect current sensor measures charge/load current.

ADC samples are oversampled, range-checked, and converted to engineering units before the controller calculates energy features. A local OLED is optional. The cloud receives timestamped summaries rather than raw high-rate samples, reducing radio-on time and preserving storage during outages.

V. HARDWARE COMPONENTS

Component selection should follow measured source characteristics. Standard piezo disks are convenient for proof-of-concept work but can have high source impedance and fragile solder joints. Beam transducers can provide more controlled strain at the cost of mechanical volume. A Schottky bridge is simple but its voltage drop can be material at low excitation; an active or synchronized rectifier may be considered only after its controller overhead is shown to be justified. The charger must be selected for low-current operation and must include the safety functions required by the cell manufacturer.

The sensing front end requires equal care. Voltage dividers should be designed so the largest clamped voltage is below the ADC input range; a small RC filter and input protection limit impulsive transients. The ESP32 ADC has nonidealities, so a multi-point calibration against a bench meter should be stored in firmware [11]. Current sensing must not impose a voltage burden large enough to alter the energy-transfer experiment. For publication, give part numbers, gains, sampling intervals, calibration uncertainty, and wiring topology.

Battery protection is non-negotiable. Piezoelectric sources are intermittent and can produce short highvoltage excursions; a safe implementation uses a specification-compliant charge controller, protection circuitry, and the cell manufacturer's limits for voltage, current, and temperature. A supercapacitor may be used ahead of a battery to accept short pulses and decouple them from charging constraints. All exposed conductive paths must be insulated and mechanically secured.

The low-power load should be characterized as a controllable duty-cycle load. For example, an LED indicator can be pulsed for a defined duration and a local display can wake only after an event. This makes energy accounting possible. Directly connecting a continuous load to the storage node is unsuitable for evaluating intermittent generation because it obscures whether missing output is caused by the harvester or by unbounded demand. A switched load, measured current path, and firmware log together provide a reproducible assessment.

Mechanical reliability is quantified through visual inspection and resistance continuity after cyclic operation. Cracked ceramic, delaminated adhesive, and cable fatigue may reduce output gradually; they are not merely manufacturing issues. Temperature and humidity also change mechanical and electrical behavior. A final prototype should report the enclosure rating, any conformal coating, and the test environment. Such evidence is particularly important if the target locations include entrances or transit facilities.

Component	Selection rationale	Design note
Piezoelectric array	Converts periodic compression to charge	Mechanically preloaded; grouped series-parallel
Bridge / clamp	Converts AC pulses and limits overvoltage	Use low-leakage, low-forward-loss devices
Reservoir + charger	Buffers pulses and controls Li-ion charging	Apply cell protection and thermal limits
ESP32	ADC, control, Wi-Fi telemetry	3.0-3.6 V supply; ADC calibration required [11]
Voltage/current sensors	Observes rails and load	Use divider protection and calibrated gain
OLED / LED load	Local status and demonstration	Enable only under energy budget

VI. AI-BASED ENERGY MANAGEMENT

The policy can be trained or configured from deployment data without maintaining a computationally expensive neural network. For example, the event-rate forecast is rhat[k] = alpha r[k] + (1-alpha) rhat[k-1], where alpha is selected from a validation period. The controller can map rhat and SoC to a finite-state policy table. Such a policy is suitable for the ESP32, explainable to maintainers, and robust when the amount of historical data is small. A more complex model is justified only if it reduces missed

reports or materially improves storedenergy utilization.

Fault handling is part of intelligent management. A sustained zero-voltage condition after detected mechanical events may indicate an open connection, whereas a persistent high rail can indicate a clamp or charger fault. The controller therefore assigns health flags, timestamps them, and reports them when radio budget permits. Decision logs should record why a transmission was deferred so an operator can distinguish energy-aware behavior from a communications failure.

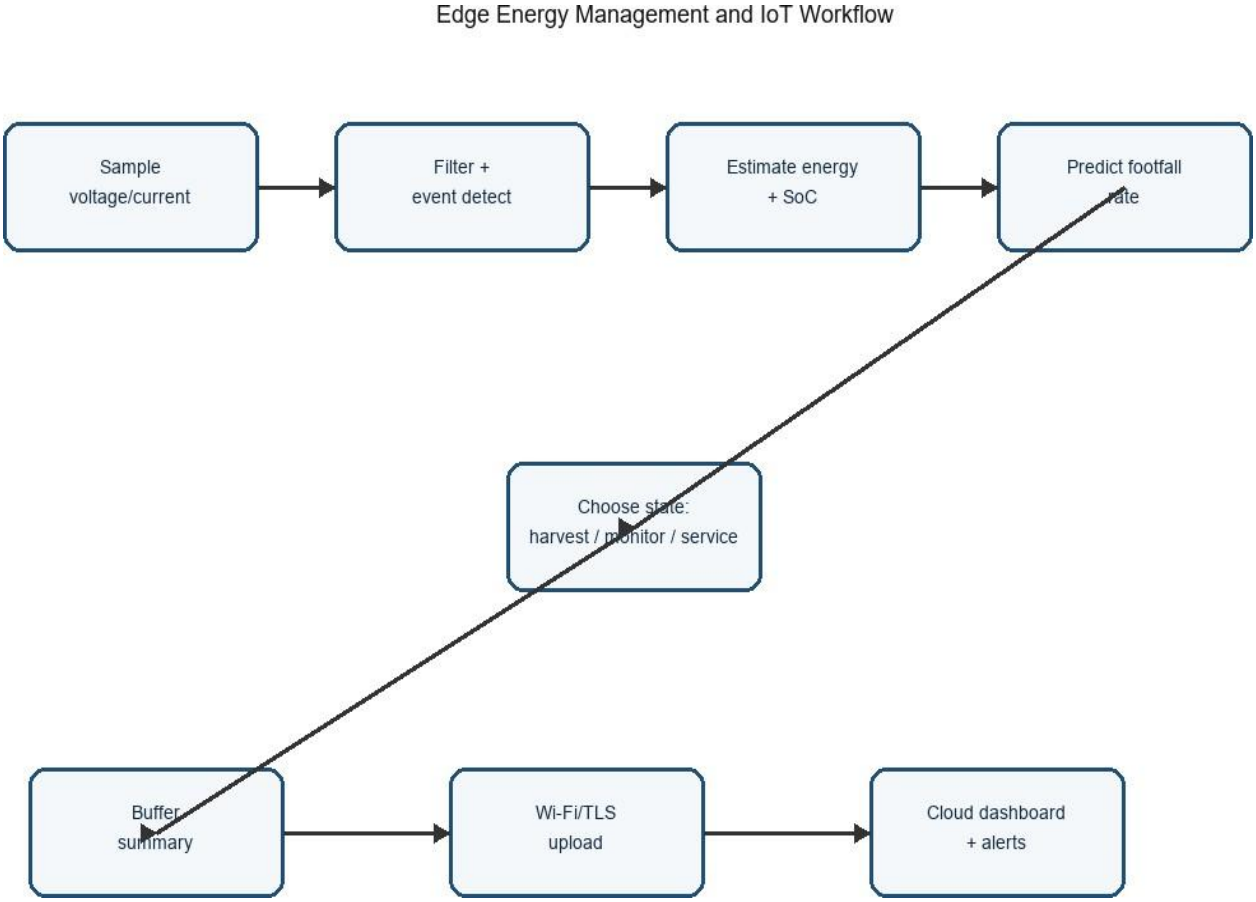


Fig. 2. AI-assisted edge energy management and IoT workflow.

The workflow executes locally and makes the cloud advisory rather than essential. A cloud dashboard can perform longer-horizon reporting, but a loss of internet access must not cause unsafe charging behavior or unnecessary battery depletion. For small experimental datasets, split data by time window rather than by random events when tuning alpha and thresholds; this prevents a future traffic pattern from leaking into the forecast evaluation.

The policy thresholds are selected from an energy ledger. Let Eu be the energy of one upload, Ed the energy of the display action, and er the reserve. The service state is entered only if stored energy exceeds Er + Eu + Ed and the predicted interval contains sufficient events. The monitor state permits sampling but defers optional actions. This simple guard prevents a visually attractive load from draining the buffer just before a fault report is required. In testing, compare this policy with a periodic-upload baseline using missed reports, time above reserve, and mean radio energy as metrics.

The term prediction should remain bounded by evidence. A short exponentially weighted forecast is appropriate for repeated pedestrian patterns such as a class-change interval, but it may be inaccurate for unusual events. The safety property must not depend on forecast accuracy: a conservative SoC threshold always overrides a positive prediction. This makes the algorithm useful even with little prior data and

prevents an optimistic model from compromising the storage reserve.

The term AI is used here in its appropriate embedded sense: a small predictive decision policy, not a powerhungry cloud model. The controller maintains a 10-min sliding window of accepted step events. Features are event count N, mean inter-arrival time, recent energy estimate, battery state of charge (SoC), and Wi-Fi availability. Exponentially weighted moving averages predict the near-term event rate. The policy places the platform in one of three states: *harvest-only* (SoC below reserve), *monitor* (local acquisition, deferred upload), or *service* (normal telemetry and LED/load permission).

Algorithm 1: Energy-aware scheduling.

At each acquisition interval, filter ADC values; estimate event energy; update SoC and event-rate estimate. If SoC < S, disable discretionary load and transmit only alarms. Min Else if predicted energy is below the next transmission budget, queue the payload and remain in monitor mode. Otherwise publish the feature packet, permit the scheduled load interval, and return to sampling. This policy is explainable, constant-memory, and testable on-device.

VII. IOT MONITORING AND WORKING PRINCIPLE

A practical payload interval is adaptive. During high traffic, the node can publish aggregate statistics at a fixed interval or after a target event count. During sparse traffic, it can transmit only when a battery threshold, fault condition, or meaningful energy delta is crossed. This event-driven workflow reduces both radio energy and cloud storage. Credentials must not be hard-coded in a public repository; encrypted transport, unique identifiers, and server-side access control are recommended for a deployable system [16]-[18].

Each record should include firmware version and calibration version in addition to electrical variables. This enables a dashboard to distinguish a physical change in tile behavior from a software update. Time synchronization may be obtained during network availability; while offline, the controller can maintain a monotonic event sequence and reconcile timestamps after reconnection. The dashboard should expose missing-data intervals rather than interpolate them as zero energy.

The dashboard should display measured units and data quality explicitly. Rectified rail voltage, buffer voltage, estimated accepted energy, event count, and battery SoC are distinct channels. A message queue can record failed publishes locally; after recovery, packets are uploaded in order with their original sequence number. The operator should see the sequence gap and sync state. This design supports auditability and prevents a temporary Wi-Fi outage from appearing as an absence of pedestrian activity.

Cloud monitoring also exposes privacy considerations. The proposed payload uses electrical event features, not images or personal identifiers. If footfall analytics are extended to occupancy estimation, only aggregate counts should be exported unless a separate ethics and privacy review authorizes richer data.

Device logs should use pseudonymous tile identifiers, and dashboard access should be restricted to authorized operators. On impact, stress in the active material creates charge. The bridge rectifier conducts, the reservoir absorbs the pulse, and the storage interface transfers energy subject to its acceptance constraints. The ESP32 samples after a settling interval; it applies a median filter to suppress impulse artefacts, aggregates min/max/mean voltage and current, and computes a quality flag. Packets contain tile identifier, timestamp, event count, estimated accumulated energy, SoC, and fault flags. MQTT or HTTPS may be used; TLS credentials should be provisioned per device. When connectivity fails, a ring buffer retains summaries for store-and-forward upload. ThingSpeak or an equivalent dashboard can render voltage, current, SoC, and event trends [12].

VIII. ALGORITHMS AND MATHEMATICAL ANALYSIS

To convert sampled quantities into an energy estimate, the firmware uses $\widehat{E} = \sum_n V_{\mathrm{b}}[n] I_{\mathrm{b}}[n] \Delta t$ over a reporting interval for the regulated/battery rail. For the pulse rail, an oscilloscope-based characterization should derive a correction relationship between the sampled peak feature and accepted storage energy. Reporting both quantities avoid confusing rectified peak voltage with energy. Measurement uncertainty arises from divider tolerance, ADC quantization, sensor gain, sampling

phase, and the mechanical repeatability of footsteps; these should be propagated or bounded in the final experiment.

The capacity-sizing calculation is equally important. For a required survival interval T and average quiescent power P_{q}, the buffer must satisfy $E_{\mathrm{usable}} \geq P_{\mathrm{q}}T$ plus the energy of one planned upload and a safety margin. For a battery with nominal voltage V_{b} and usable fraction β, a first estimate is $C_{\mathrm{bat}} \geq \frac{E_{\mathrm{usable}}}{\beta V_{\mathrm{b}}}$. This is a planning equation, not a substitute for cell characterization, because temperature, aging, and converter efficiency reduce the usable capacity.

For a piezoelectric element with effective piezoelectric coefficient d, electrode area A, applied normal force F, and thickness t, a first-order charge model is $Q = dF$. The element capacitance is $C_{\mathrm{p}} = \frac{\varepsilon_0 \varepsilon_{\mathrm{r}} A}{t}$; hence the ideal open-circuit voltage is $V_{\mathrm{oc}} = \frac{Q}{C_{\mathrm{p}}}$. This voltage is not a load-power claim: rectifier threshold, leakage, source capacitance, and the mechanical waveform determine delivered energy.

For an approximately sinusoidal source, a useful electrical abstraction is a current source I_{p} in parallel with the source capacitance C_{p}. With angular frequency ω and resistive load R, the RC output amplitude is $V_{\mathrm{out}} = \frac{I_{\mathrm{p}}R}{\sqrt{1+(\omega RC_{\mathrm{p}})^2}}$, and the average power is $P = \frac{{V_{\mathrm{rms}}}^2}{R}$. The energy added to the storage capacitor is $\Delta E = \eta \cdot \frac{1}{2} C_{\mathrm{store}}\left({V_2}^2 - {V_1}^2\right)$, where η includes conversion and charging loss. In sampled operation, $E[k] = E[k-1] + E_{\mathrm{harv}}[k] - E_{\mathrm{load}}[k] - E_{\mathrm{q}}[k]$. The energy manager permits a task only if $E[k]$ exceeds the task budget plus a reserve margin. These equations are consistent with standard piezoelectric modelling and interface analyses [8]-[10], [13].

IX. EXPERIMENTAL RESULTS AND DISCUSSION

The analytical variability in Fig. 2 illustrates a key practical point: nominally similar steps do not produce identical charge transfer. Force, foot placement, cadence, contact duration, and tile mechanics alter the waveform. For this reason, a future experimental paper should plot distributions instead of a single maximum voltage. It should state whether values are instantaneous peaks, RMS values, power across a specified load, or energy accepted by storage. These quantities answer different questions and cannot be substituted for one another.

Energy neutrality should also be evaluated. Let Eharv, d be the median daily accepted energy and Ectrl, d the controller, sensing, display, and radio energy. Continuous autonomous operation requires Eharv, d greater than Ectrl, d plus a reserve for low-traffic periods. If this inequality is not met, the system remains useful as a hybrid sensor tile, but auxiliary power must be declared. This framing protects the scientific credibility of the technology and gives designers a transparent deployment criterion.

A recommended results layout has three parts. The first reports mechanical input: force, displacement, cadence, and tile geometry. The second reports electrical conversion: waveform, loaded voltage, current, energy, and storage efficiency. The third reports system behavior: sampling availability, upload success ratio, per-upload energy, and battery trajectory. Separating these layers allows another laboratory to reproduce a failure or success without guessing whether the cause was mechanical, electrical, or software-related.

The validation plan includes a no-load test, loaded resistor sweep, capacitor charge test, and complete system endurance run. In the resistor sweep, select loads around the estimated source impedance and measure voltage and current concurrently. In the capacitor test, calculate energy from the change in squared voltage, which is more reliable than using a short peak. In the complete-system run, document every active peripheral so that observed battery behavior can be attributed to the correct component.

Statistical reporting should include sample size, central tendency, dispersion, and excluded trials with justification. A high maximum can be retained as an observation but should not be presented as typical performance. Plotting force or displacement against accepted energy will reveal the mechanical operating range. Reporting calibration method and uncertainty gives readers a basis for judging whether apparent performance differences are physically meaningful.

Evidence status:

The supplied source report specifies components but provides no calibrated voltage/current/time series.

Consequently, Table II and Fig. 2 are an *analytical validation example*, constructed from the above model to show expected variability and the calculations that a laboratory evaluation must reproduce. They must be replaced with measured, instrument-traceable values before publication. This explicit separation prevents open-circuit peaks from being misrepresented as harvested power.

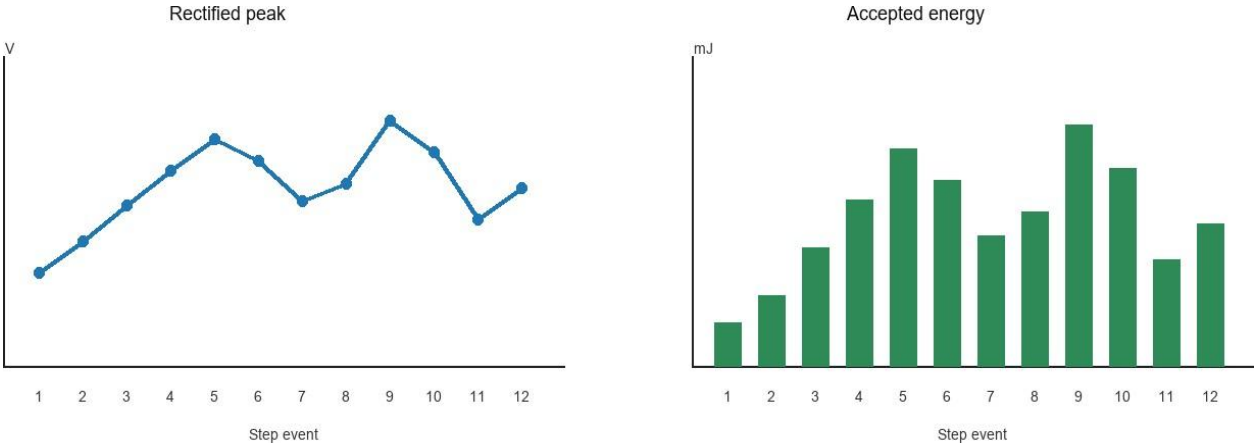


Fig. 2. Analytical per-event response for a representative validation scenario; not claimed as measured prototype data.

Metric	Analytical scenario	Interpretation
Rectified peak voltage	2.1-5.5 V per event	Force and contact placement drive variance
Estimated accepted energy	0.11-0.61 mJ per event	After assumed conditioning losses
12-event accumulated energy	4.49 mJ	Insufficient for continuous Wi-Fi operation
Recommended telemetry mode	Event aggregation	Upload only after energy/interval threshold

A bench experiment should use a repeatable actuator or instrumented mass, oscilloscope voltage traces across a known load, synchronized current logging, and at least 30 repetitions at each force level. Report median, interquartile range, source impedance, storage efficiency, and all loads active during tests. A separate endurance test should include at least 10,000 cycles, while communication testing should measure radio energy per successful upload. This protocol turns the present publication draft into a falsifiable study rather than a demonstration narrative.

X. COMPARATIVE ANALYSIS

Table III compares architectural emphasis rather than claiming a direct numerical ranking, because published tile dimensions, excitation, load resistance, and measurement locations are not standardized. The proposed system is differentiated by energy-aware scheduling and measurement transparency. Its performance claim should be evaluated after prototype trials using the common reporting fields described above, not by comparing its open-circuit voltage against another study's loaded power result.

For fair comparison, normalize energy by both event count and active area where appropriate, and state whether a load is continuously attached. A system that lights an LED briefly may be compelling as an interaction demonstration yet have a very different energy profile from one that sustains an environmental sensor. The comparison table therefore favours design attributes and reporting discipline over headline voltage values.

Approach	Energy conditioning	Monitoring	Practical limitation
Basic disk prototype	Bridge + capacitor	None	Voltage-only demonstrations
Tile/beam harvester [5],[6]	Optimized mechanical structure	Limited	Site-dependent output
IoT smart floor [7]	Hybrid / buffered	Cloud sensing	May require auxiliary supply
This work	Protected buffer + energy policy	ESP32, store-forward	Requires measured validation

XI. ADVANTAGES, APPLICATIONS, AND FUTURE SCOPE

For a public installation, value can be communicated honestly: a display may show real-time footfall and accumulated stored energy while explaining that each tile supports low-power sensing or signalling. This is more defensible than promising grid-scale energy. The modular electronics compartment also permits maintenance without removing the tile surface, a relevant advantage in schools, stations, museums, and controlled-access corridors.

The proposed approach offers modular installation, remote observability, energy-aware load scheduling, and clear separation between harvested energy and monitoring consumption. Suitable applications include interactive displays, low-duty-cycle occupancy sensing, educational renewable-energy installations, wayfinding indicators, and smart-city footfall analytics. It is most useful where local engagement or sensing is valuable; it should not be marketed as a high-yield power plant.

Future work should compare piezoelectric disks, beam structures, and hybrid electromagnetic designs under the same mechanical boundary conditions; investigate synchronized or active rectification; add supercapacitor buffering; use federated anomaly detection across tiles; and publish full raw datasets. Lead-free piezoelectric materials, waterproof mechanical packaging, cybersecurity hardening, and lifecycle cost assessment are also necessary before large-scale deployment.

XII. CONCLUSION

This paper has defined a complete, energy-aware smartfootstep platform based on piezoelectric transduction, storage buffering, ESP32 control, and cloud monitoring. The design treats energy harvesting as a constrained system problem, not merely a high-voltage sensor output. A lightweight predictive policy protects battery reserve and schedules telemetry according to expected energy availability. The included calculations and validation protocol provide a defensible route to measurement. The proposed platform can support lowduty-cycle sensing and visible smart-infrastructure functions in high-footfall environments, subject to rigorous prototype characterization before any deployment or publication claim.

REFERENCES

[1] J. B. N. et al., “Available technologies and commercial devices to harvest energy by human trampling in smart flooring systems: A review,” *Energies*, vol. 15, no. 2, Art. no. 432, 2022.

[2] S. Priya and D. J. Inman, Eds., Energy Harvesting Technologies. New York, NY, USA: Springer, 2009.

[3] A. Erturk and D. J. Inman, Piezoelectric Energy Harvesting. Chichester, U.K.: Wiley, 2011.

[4] H. A. Sodano, D. J. Inman, and G. Park, “A review of power harvesting from vibration using piezoelectric materials,” Shock and Vibration Digest, vol. 36, no. 3, pp. 197–205, 2004.

[5] X. Zhang et al., “Design and comparative study of a small-stroke energy harvesting floor based on a multi-layer piezoelectric beam structure,” Micromachines, vol. 13, no. 5, Art. no. 736, 2022.

[6] M. M. El-Sayed et al., “Human footsteps-based energy harvesting using piezoelectric elements,” in Proc. IEEE ITC-Egypt, 2023, pp. 140–144, doi: 10.1109/ITC-Egypt58155.2023.10206103.

[7] A. K. et al., “An IoT-enabled piezoelectric smart floor for footfall monitoring, energy harvesting, and anomaly detection at a bus terminal,” Engineering Science and Information Systems, vol. 31, no. 5, 2026.

[8] Y. Shu and I. C. Lien, “Analysis of power output for piezoelectric energy harvesting systems,” Smart Materials and Structures, vol. 15, no. 6, pp. 1499–1512, 2006.

[9] D. Guyomar, A. Badel, E. Lefeuvre, and C. Richard, “Toward energy harvesting using active materials and conversion improvement by nonlinear processing,” IEEE Transactions on Ultrasonics, Ferroelectrics, and Frequency Control, vol. 52, no. 4, pp. 584–595, 2005.

[10] H. Lallart and D. Guyomar, “An optimized self-powered switching circuit for non-linear energy harvesting with low voltage output,” Smart Materials and Structures, vol. 17, no. 3, 2008.

[11] Espressif Systems, “ESP32 series datasheet,” ver. 5.2, 2025. [Online]. Available: ESP32 Series Datasheet

[12] MathWorks, "ThingSpeak IoT analytics," 2025. [Online]. Available: ThingSpeak IoT Analytics
[13] Y. Chen, Y. Wang, and S. Zhou, "Piezoelectric energy harvesters: An overview on design strategies and topologies," IEEE Access, vol. 10, pp. 120133–120157, 2022.
[14] B. Zhao, F. Qian, A. Hatfield, L. Zuo, and T.-B. Xu, "A review of piezoelectric footwear energy harvesters: Principles, methods, and applications," Energy Harvesting and Systems, 2023.
[15] M. A. M. et al., "Piezoelectric sensors as energy harvesters for ultra-low-power IoT applications," Sensors, vol. 24, no. 8, Art. no. 2587, 2024.
[16] IEEE, IEEE Standard for Low-Rate Wireless Networks, IEEE Std. 802.15.4-2024, 2024.
[17] OASIS, MQTT Version 5.0, OASIS Standard, 2019.
[18] National Institute of Standards and Technology (NIST), Considerations for Managing Internet of Things (IoT) Cybersecurity and Privacy Risks, NISTIR 8228, 2019.
[19] C. R. Saha, T. O'Donnell, H. Lefeuvre, P. H. W. Leung, and S. G. Roy, "Electromagnetic generator for harvesting energy from human motion," *Sensors and Actuators A: Physical*, vol. 147, no. 1, pp. 248–253, 2008.
[20] M. Ferrari, V. Ferrari, M. Guizzetti, B. Andò, S. Baglio, and C. Trigona, "Improved energy harvesting from wideband vibrations by nonlinear piezoelectric converters," *Sensors and Actuators A: Physical*, vol. 162, no. 2, pp. 425–431, 2010.
[21] A. Harb, "Energy harvesting: State-of-the-art," *Renewable Energy*, vol. 36, no. 10, pp. 2641–2654, 2011.
[22] S. Usha, P. Rajeshwar, S. S. Kumar, K. Yeswanth, and G. Yugesh, "Review of piezoelectric energy harvesting through footsteps," *International Journal of Composite Constituent Materials*, 2023.
[23] R. D. B. et al., "A review of piezoelectric energy harvesting tiles: Available designs and future perspective," *Energy Conversion and Management*, vol. 254, Art. no. 115272, 2022.
[24] A. Khalil et al., "Smart city applications of piezoelectric energy harvesting: A survey," *Smart Cities*, vol. 7, no. 2, pp. 1–22, 2024.
[25] Allegro MicroSystems, "ACS712 fully integrated, Hall-effect-based linear current sensor IC," datasheet, 2024.